MPhys Project: Simulating Spin Ice and Other Ising Magnets Using Monte Carlo Methods

Candidate number: 1023902 Project number: CMP15 Supervisor: Prof S. J. Blundell

Abstract

Monte Carlo simulations of spin ice and other magnetic Ising models are presented. Typical properties of spin ice are shown including signature characteristics of magnetic monopole excitations. Monopole noise simulations produce dynamics which agree qualitatively with experiment and are mostly consistent with other studies. Properties of Monte Carlo simulations such as finite size effects and critical behaviour were also investigated.

1 Introduction

Condensed matter systems have proven to be excellent laboratories for studying quantum and statistical mechanics and often show that some of the most profound phenomena in physics can only be understood as emergent properties. The class of exotic magnets known as spin ice is no exception to this rule. Spin ice is so called as it is a magnetic analogue of water ice, and was also the first ferromagnetic system known to exhibit geometric frustration; both these properties have attracted intense interest, but the understanding of spin ice was revolutionised when it was realised that below 10 K the spin magnetic dipoles fractionalise into deconfined magnetic monopoles which interact with a magnetic equivalent of Coulomb's law. Other instances of fractionalisation, such as the fractional quantum Hall effect, are rare and often occur as a result of low dimensionality, but magnetic monopole excitations are observed even in bulk 3D spin ice. Fundamental magnetic monopoles have never been detected despite exhaustive experimental searches, so their emergence in spin ice serves to exemplify the power of condensed matter physics to reveal phenomena which remain elusive to the fundamental approach. Although the monopole picture has been highly successful in accounting for the magnetic properties of spin ice materials, their dynamics have been found to display correlations which are yet to be fully understood.

In this project I will use Monte Carlo simulations to study various phenomena in the spin ice regime such as the structure of the ground state, the magnetic properties and low temperature monopole dynamics. The focus is on qualitatively reproducing spin ice properties, but some quantitative contact with experiment is made in the study of magnetic monopole generation-recombination. I also studied some simpler systems such as the well-known 3D Ising model, which I used to investigate the behaviour of the simulation, and a 2D analogue of spin ice known as 'square ice' with non-interacting monopole excitations.

2 Theory

2.1 Fundamentals of spin ice

The canonical spin ice compounds, principally including dysprosium titanate ($Dy_2Ti_2O_7$) and holmium titanate ($Ho_2Ti_2O_7$), consist of lanthanide ions with large magnetic moments (about $10\mu_B$ for Dy^{3+} and Ho^{3+}) situated at the intersections of a lattice of corner sharing tetrahedra (the pyrochlore lattice, see figure 1a). The other ions in the crystal are non-magnetic but create a crystal field which constrains the spin ground states of the individual lanthanide ions to be almost a pure doublet with $|J\ M_J\rangle = |J\ \pm J\rangle$ pointing in and out of the tetrahedra (along the [111] crystallographic axes). Higher crystal field levels lie hundreds of Kelvin above the grounds state and are not thermally accessed below ≈ 10 K, so that the spins are exceptionally well approximated by classical Ising spins in this temperature regime [5, 19]. As a result the spins can never be configured to satisfy the effective ferromagnetic interaction, giving rise to geometric frustration.

In the spin ice ground state each tetrahedron has two spins pointing in and two pointing out. This condition is known as the 'ice rule' and gives rise to a macroscopically degenerate ground state, so called because the number of ways of satisfying the ice rules increases with the system size. This ground state was found by Linus Pauling in 1935 to describe low temperature water ice [28], which remains the paradigm for understanding spin ice. The correspondence between spin ice and the analogous behaviour in water ice is summarised in table 1. In the I_c phase in water ice, oxygen atoms form a diamond lattice with hydrogen nuclei (protons) lying in between neighbouring pairs of oxygen atoms. Each oxygen atoms has two covalently bonded protons and is hydrogen bonded to two further protons; the covalently bonded protons sit much closer to the oxygen atom than the hydrogen bonded ones. Thus in the ground state each oxygen atom has four neighbouring protons with two close by and two further away. The I_c phase maps onto the spin ice structure easily since the centres of the tetrahedra in the pyrochlore lattice form a diamond lattice; likewise the bond midpoints in a diamond lattice form a pyrochlore lattice. In this way the tetrahedron centres in spin ice in the ground state with two spins pointing in and two pointing out can be likened to oxygen atoms in water ice with two nearby protons and two farther protons; low-lying excitations involve '3 in-1 out' and '1 in-3 out' states which are created by a spin flip in spin ice or a proton hopping in water ice.

Spin ice and water ice share many important properties. Pauling predicted that the macroscopically degenerate ground state would give rise to a non-negligible entropy [28], and this was confirmed by contemporary experiments [16]. Likewise the ground state entropy of spin ice was measured by comparing

	Spin ice	Water ice (I_c phase)
Diamond Structure	Tetrahedron centres	Oxygen atoms
Pyrochlore Structure	Tetrahedron corners (where spins are)	Midpoints between neighbouring oxygens
Degrees of freedom	Spin orientations	Proton positions
Allowed configurations	Spins point into/ out of tetrahedra	Protons sit closer to one oxygen
Ground state	Tetrahedra have 2 in-2 out spin configuration	Each oxygen has 2 near protons
Exciations	Spin flips	Proton hops to neighbouring oxygen
Fractional-isation phenomenon	Deconfined monopoles	Dissociated H_3O^+ OH^- pair

Table 1: Comparison of spin ice structure and phenomena with analogues in I_c water ice.

the discrepancy in the integrated heat capacity with the high temperature paramagnetic entropy, and the result agrees with Pauling's value [29]. We will see that the macroscopically degenerate ground state has consequences for the magnetic properties of spin ice. Furthermore, Pauling showed that water ice can switch between ground states or equivalent excited states with no energy cost by identifying a loop of similarly aligned protons and simultaneously moving all of them; furthermore, if the ice rules are broken on one site, the defect can be transferred to another site by the hopping of a proton. Spin ice can also change between this states in this way, which we will see allows the propagation of magnetic monopole excitations. A related issue is that spin ice fails to relax to an ordered state with zero entropy at low temperature either in experiments or Monte Carlo simulations, despite the use of loop algorithms in some simulations to facilitate switching between ground states[1] [17] [21]. The only way to square this behaviour with the third law of thermodynamics is if the characteristic relaxation time diverges at low temperature [3]. This has been observed in experiments and simulations, including the one presented here [12, 19].

2.2 Magnetic monopole excitations

Spin ice contains both an antiferromagnetic superexchange interaction between nearest neighbour lanthanide ions and a dipolar interaction; unusually due to the strong lanthanide ion magnetic moments these interactions are comparable in strength, which leads to the effective ferromagnetic behaviour [5]. This leads to the dipolar spin ice (DSI) Hamiltonian for spins $\mathbf{S}_i$ separated by $\mathbf{r}_{ij}$

$$H = -J\sum_{\langle i,j\rangle}\mathbf{S}_i\cdot\mathbf{S}_j + \frac{\mu_0\mu^2}{4\pi}\sum_{i<j}\left(\frac{\mathbf{S}_i\cdot\mathbf{S}_j}{r_{ij}^3} - \frac{3(\mathbf{S}_i\cdot\mathbf{r}_{ij})(\mathbf{S}_j\cdot\mathbf{r}_{ij})}{r_{ij}^5}\right) \quad (1)$$

[1]This is often referred to as 'glassy' behaviour.

where μ is the lanthanide magnetic dipole moment and J is the exchange interaction strength. The first term sums over nearest neighbours $\langle i,j\rangle$ whilst the second term is the usual dipolar energy. It was initially unclear why the relatively strong long range dipolar interaction failed to destroy the disordered ice ground state and produce an ordered state [5]. A paradigm shift from a dipolar to a monopolar Hamiltonian resolved this conundrum. [7].

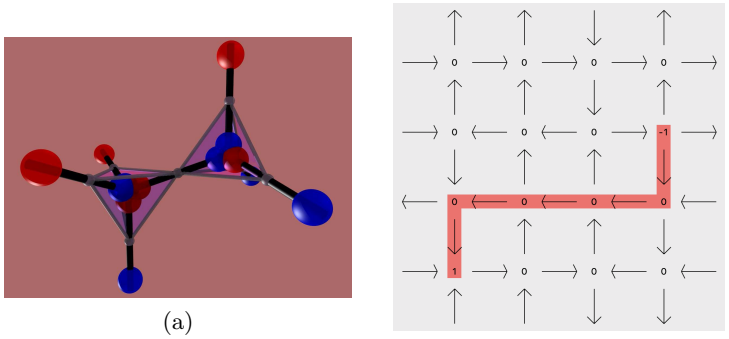

(a) (b)

Figure 1: (a) Schematic diagram of two pyrochlore tetrahedra with spins (shown as dumbbells) sitting on the corners. The magnetic charge on each tetrahedron is the sum of the dumbbell charges contained within it. Reproduced from ref. [7] (b) Schematic diagram of a Dirac string in square ice (a 2D equivalent of spin ice) connecting two monopole excitations, whose charges are denoted by the numbers at the sites. Note that in general there can be more than one Dirac string connecting two monopoles.

Here is a sketch of how this comes about, following the one in ref. [7]. Consider a picture of a magnetic dipole as a 'dumbbell' with two oppositely charged magnetic monopoles separated by a distance a_d (as in an electric dipole). The magnetic monopoles are sources and sinks of the magnetic field $\mathbf{H}$ and their charges will be $q_m = \pm\mu/a_d$. A pyrochlore tetrahedron in the 2 in-2 out ground state contains two north poles and two south poles[2], so by Gauss' theorem it has no net flux of $\mathbf{H}$ leaving its surface. If a spin is flipped this puts one tetrahedron in a 3 in-1 out state and a neighbouring one in a 1 in-3 out state, so that the former has a south pole swapped for a north pole, giving it a net magnetic charge $Q = 2\mu/a_d$, and vice versa for the latter. In this way the pyrochlore tetrahedra where the ice rule is broken are sources or sinks of $\mathbf{H}$. These ideas are applicable to any magnetic material, but spin ice is unique because a further spin flip can transfer the magnetic charge to a neighbouring tetrahedron without any further violations of the ice rule (only changes in the dipolar energy), allowing magnetic monopoles to hop between tetrahedra. In this way spin ice can be viewed as a lattice gas with a diamond structure where magnetic monopoles with charge Q are created in pairs on adjacent sites and hop between sites. The dumbbell picture of dipoles is mapped to the lattice gas picture of spin ice using $Q_\alpha = \sum q_m^i$ where q_m^i are the dumbbell charges which sit inside the tetrahedron α. Doubly charged monopoles can also be created by flipping two in or out spins on a site, placing four north or four south poles inside a tetrahedron.

[2]With the terms north and south pole I am referring to positive and negative magnetic charges respectively.

The Coulomb interaction between charges in electric dipoles produces an electric dipole interaction energy equivalent to the second term in equation (1), which is exact in the limit of point dipoles (see for example ref. [18]). Hence in the dumbbell picture the dumbbell charges on different tetrahedra will have a Coulomb interaction energy proportional to $q_m^i q_m^j / r_{ij}$. The corrections are small, fall off as $1/r^5$ and have been shown using Monte Carlo simulations to be inconsequential [7, 19]. Furthermore, to reproduce the nearest neighbour exchange interaction, the dumbbell charges will have an interaction proportional to $q_m^i q_m^j$ when they are in the same tetrahedron (clearly a $1/r$ interaction is ill-defined in this case). Switching from the dumbbell picture to the lattice gas picture and ignoring the dumbbell self-energy (which is a constant correction) gives the monopolar spin ice Hamiltonian

$$H = \frac{1}{2}\nu_0 \sum_\alpha Q_\alpha^2 + \frac{\mu_0}{4\pi} \sum_{\alpha<\beta} \frac{Q_\alpha Q_\beta}{r_{\alpha\beta}^2} \tag{2}$$

where Q_α are the magnetic monopole charges on diamond lattice sites α (details of this step are in the supplement to ref. [7]). It is now easy to see that the ground state will be governed by the ice rule since this involves setting $Q = 0$ on all sites (the first term is always positive and will be stronger than the second term in spin ice materials). Setting the energy required to create a monopole pair ν_0 to be

$$\nu_0 \left(\frac{\mu}{a_d}\right)^2 = \frac{J}{3} + \frac{4D}{3}\left(1 + \sqrt{\frac{2}{3}}\right) \tag{3}$$

correctly reproduces the exchange interaction. The Hamiltonian (2) shows that excitations can be viewed as monopoles which have charge Q and are deconfined because they can be separated to infinity with a finite energy cost, making them *bona fide* emergent particles rather than just bound charges.

2.3 Monopole dynamics

At first glance it seems as though magnetic monopoles in spin ice will behave as a Coulombically interacting plasma which undergoes stochastic generation-recombination (GR) at finite temperature (albeit one where monopoles are restricted to sit on diamond lattice sites). Such a system can be modelled with the Langevin equation

$$\frac{\mathrm{d}(\delta N)}{\mathrm{d}t} = -\frac{\delta N}{\tau(T)} + A(T)\zeta(t) \tag{4}$$

where the number of monopoles N fluctuates about the mean $N_0(T)$ as $\delta N = N - N_0$ with a characteristic GR time τ which depends on the temperature [12]. The first term represents the exponential relaxation to the mean whilst the second term is a random fluctuation which is uncorrelated in time and also depends on temperature. The power spectral density of monopole number fluctuations is given by the Wiener-Khinchin theorem [30] as the Fourier transform of the autocorrelation of the fluctuations

$$S_N(\omega) = \int_0^\infty 4\cos\omega t \; C_N(t) \; \mathrm{d}t \tag{5}$$

where the autocorrelation is defined as

$$C_N(t) = \frac{1}{W}\int_{-1/W}^{1/W} \delta N(t') \; \delta N(t'+t) \; \mathrm{d}t'. \tag{6}$$

This yields the Debye-Lorentzian form

$$S_N(\omega) = \frac{4{\sigma_N}^2\tau}{1+(\omega\tau)^2} \tag{7}$$

where ${\sigma_N}^2$ is the variance of the fluctuations, which is expected to be independent of temperature in much of the spin ice regime [12]. This describes a GR noise spectrum with constant power at low frequencies (on longer timescales than the GR timescale τ) and a power law fall off on timescales below τ (where the system becomes a free plasma with no GR) and a transition on the order of $\omega = 1/\tau$. This noise spectrum can be both measured experimentally and simulated with Monte Carlo simulations (as I have done in this project), and its properties can be used to understand the timescale and nature of monopole dynamics [12].

This view is a good approximation and has succeeded to a great extent in describing monopole dynamics, but there are complications. The Langevin equation (4) assumes that the motion of the monopoles is uncorrelated, but in fact topological constraints exist which show that the picture of monopoles hopping freely constrained only by a Coulomb interaction is incomplete [12, 27]. When a monopole pair is created and subsequently separates, a chain of dipoles pointing from north to south is created. This is known loosely as a Dirac string, after the objects which connected fundamental magnetic monopoles in Dirac's theory[3] [10]. However, this means that monopoles can only recombine by traversing a Dirac string which connects them. If two oppositely charged monopoles arrive on neighbouring sites without doing so, flipping the spin connecting the tetrahedra will not recombine the monopoles but create a doubly charged pair. It has been suggested that this can lead to a 'dynamical arrest' where two oppositely charged monopoles come into contact thanks to their mutual Coulomb interaction but cannot recombine, instead having to overcome their mutual attraction in order to re-traverse the Dirac string [8]. Experiments have found that monopole dynamics can be better described by two characteristic time constants differing by about an order of magnitude, with the origin of the longer one attributed to this dynamical arrest [24]. More generally, a monopole may only move to three of the four neighbouring tetrahedra, because the fourth move creates a doubly charged monopole (a 4 in or 4 out state) rather than restore the ice rules on the first tetrahedron [19]. Yet another issue is that the initial DSI Hamiltonian (1) is not exact because it takes into account only nearest neighbour superexchange between lanthanide spins, but there will be next nearest neighbour interactions which are small but non-negligible and would be very hard to account for with Monte Carlo simulations in the monopole picture. This effect is hinted at by the fact that unexplained spin correlations appearing in neutron scattering experiments are more pronounced in $Dy_2Ti_2O_7$, which has the larger exchange interaction, than in $Ho_2Ti_2O_7$ [14].

[3] In Dirac's theory of fundamental magnetic monopoles, the magnetic charges lie at the ends of wavefunction nodes known as Dirac strings and must be quantised in order to ensure that these strings are unobservable [10]. By contrast, in spin ice the Dirac strings have been observed in neutron scattering experiments [27], and the monopole charge is not quantised but is in fact tuneable using hydrostatic pressure due to its dependence on the lattice constant [7].

The effect of topological constraints is expected to be minimal in the low frequency regime where GR noise appears 'white', but will affect the power law drop-off in the high frequency regime. To deal with this one can replace the Lorentzian value of -2 with a fitting parameter $-b$, so that the GR power spectral density takes the form

$$S_N(\omega) = \frac{4{\sigma_N}^2\tau}{1+(\omega\tau)^b}. \tag{8}$$

It is generally found that $b < 2$ and decreases with temperature, but results from Monte Carlo simulations fail to agree with experiment [11, 12]. It has been suggested that the increasing deviation from the Lorentzian value at higher temperature is due to the monopole plasma becoming increasingly less sparse and spin flips which are more costly in energy beginning to compete with monopole propagation [21]. However, it remains unclear how the effects of spin correlations can be accurately represented in Monte Carlo simulations.

One experimental technique which was originally used to search for fundamental monopoles [6] is detection with a superconducting quantum interference device (SQUID): when a monopole passes through a SQUID loop a persistent current is created. This has been used very successfully to measure monopole noise in $Dy_2Ti_2O_7$ with a characteristic timescale in the millisecond range [11, 12]. I have qualitatively reproduced the behaviour of the monopole noise time constant in this range using Monte Carlo simulations. Another technique of interest is muon spin rotation (μSR), where the spins of muons implanted in a substance precess around a superposition of an internal and applied magnetic field, revealing information about the direction and time dependence of these fields as the muons decay [1]. This technique was used to measure the magnetic monopole charge in spin ice using the magnetic analogue of the Wien effect in an electrolyte [4]. However, it is not the internal fields in spin ice which give rise to a signal in μSR but the stray field just outside the sample [2]. I have created a simulation of the stray field in spin ice which could in principle be useful for interpreting the results of such experiments.

3 Methods

I used a Monte Carlo method known as the Metropolis algorithm to simulate the bulk properties of spin ice. In statistical mechanics a mean thermodynamic quantity A is obtained by summing its value in each configuration α of the system with a Boltzmann factor weight:

$$\langle A\rangle = \frac{1}{Z}\sum_\alpha A_\alpha \exp\left(-\frac{E_\alpha}{k_BT}\right) \tag{9}$$

It is impractical to compute this quantity directly for even microscopic systems, so instead one can estimate its value by sampling a number of configurations and calculating their associated thermodynamic quantities. The standard Monte Carlo approach to this is to choose configurations randomly and weight them with a Boltzmann factor, but configurations with a high energy (and therefore a low Boltzmann weight) are most likely to be chosen, meaning that a large number of configurations would have to be chosen to investigate low energy states. Hence this method would be unfeasible at low temperatures [26, 32]. Metropolis *et al.* [26] propose an alternative method which is as follows: one places the system in a random configuration before considering each particle in succession and calculating the change in the energy of the system ΔE associated with somehow changing the state of that particle. The change is performed if energy is saved, whilst if there is an energy cost to the change it is performed with a Boltzmann factor probability $\exp(-\Delta E/k_BT)$. It is shown in ref. [26] that this method chooses configurations α with probability $\exp(-E_\alpha/k_BT)$ which is much more useful at low temperatures.

The Metropolis algorithm applied to systems of Ising spins consists of sweeping the lattice and considering the energy change associated with changing each spin. The lattice is initially generated in a random state but can be cooled slowly by running the Metropolis algorithm, reducing the temperature by a small step and repeating. Furthermore, one can average over several iterations of the Metropolis algorithm per temperature step. If enough temperature steps and Metropolis iterations are used the system will reach the equilibrium ground state and elementary excited states so that their properties can be studied. Initially I studied spin ice systems using only the first term in the Hamiltonian (2), encoding the energy cost of creating monopoles but not the Coulomb interaction, because calculating the energy change on a site with only a nearest neighbour interaction was significantly less computationally intensive, making the simulations much more practical to run on a personal computer. However, the simulations presented of 3D spin ice also include the magnetic Coulomb interaction in order to make the them comparable with other simulations.

It is important to include enough temperature steps and iterations in order for the system to remain in thermodynamic equilibrium during cooling. More temperature steps are needed as the size of the lattice is increased [32]. To account for this I investigated the effect of the number of steps on the low temperature state reached by a 2D spin ice system, and the effect of the finite lattice size on the temperature where the ground state was reached for a fixed number of steps. In this way I ascertained how slowly the system needed to be cooled to reach the spin ice regime for a given lattice size.

To visually represent the low temperature properties of spin ice (an initial aim of the project) I created a program which plotted schematic diagrams of spin ice lattices using the simulation output, as well as a mini animation. These were useful for observing the structure of the ground and low-lying excited states, as well as testing various aspects of the simulation. I also tested my simulations by calculating energies of large numbers of randomly generated lattices and checking that the distributions matched qualitatively with the expected distributions based on the geometry.

I was mostly interested in bulk properties and wished to avoid effects due to termination at a surface which may affect thermodynamic properties or produce other spurious results, so I used periodic boundary conditions in all directions throughout. In the standard 3D Ising model termination significantly impacts the thermodynamic properties of microscopic simulations [23] but are not relevant to bulk properties, so they should be ignored. It is plausible that edge effects in spin ice could affect the stray field (if not the bulk properties), but the current level of understanding of these is sketchy and doesn't provide predictions which could be useful in interpreting experimental

results, so it does not make sense to include them and risk introducing spurious behaviour [21]. Simulations with periodic boundary conditions have nonetheless been used successfully to predict experimental results involving measurement of flux [12]; in addition edge effects can be mitigated experimentally by averaging over measurements using samples cleaved along different crystallographic planes [21].

4 Results and Discussion

4.1 3D Ising ferromagnet

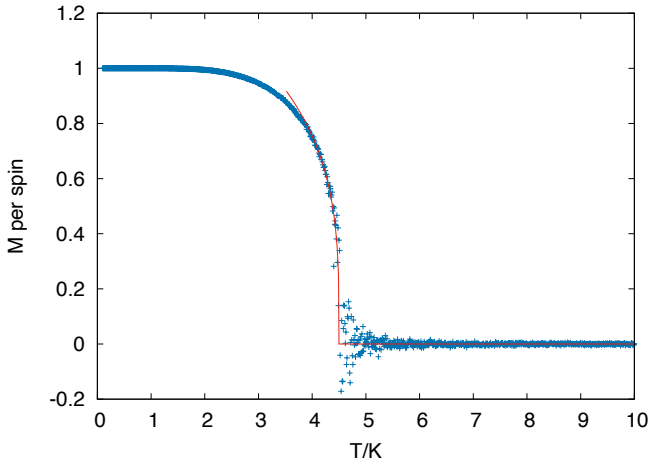

Figure 2: Monte Carlo simulations of the magnetisation a 3D Ising ferromagnet undergoing a phase transition on cooling from a paramagnetic to a ferromagnetic phase, fitted to a model with the form of equation (11) in the critical region. Typically unstable behaviour is seen in the critical region, where the characteristic spin correlation length diverges.

The general machinery developed to simulate Ising model systems was first applied to the 3D Ising ferromagnet on a simple cubic lattice with the spin axis aligned with the z axis. This was a useful exercise in checking that the system worked using a well studied model, and also for gaining insight into the finite size effects which are associated with Monte Carlo simulations. The system was simulated in zero applied field with the Hamiltonian

$$H = -J \sum_{\langle ij \rangle} s_i s_j \tag{10}$$

between 0.1 K and 10 K with $J/k_B = 1$ K. A sample made up of $16 \times 16 \times 16$ spins with periodic boundary conditions in all directions was cooled with 10^3 temperature steps and 50 iterations of the Metropolis algorithm per step. Figure 2 shows the magnetisation (which is the relevant order parameter) simulated as a function of temperature. A clear phase transition from the paramagnetic phase with $M = 0$ to the ferromagnetic phase (with all spins aligned with each other) is displayed, and the results of similar simulations in ref. [23] are reproduced. To find the critical temperature T_C the magnetisation data in the critical region were fitted to a curve of the form

$$M = \begin{cases} 0 & T > T_C \\ CN^{-\beta/\nu}\left(\frac{T_C - T}{T_C}\right)^{\beta} & T < T_C \end{cases} \tag{11}$$

where β is the critical exponent for the order parameter, $\nu = 0.63$ is the critical exponent for the correlation length [23], $N = 4096$ is the number of particles in the simulation and C is a constant. The critical temperature was found from the simulation to be 4.51 ± 0.01 K, which agrees perfectly with the best theoretical value currently available [15].

Typically a critical exponent law $M \propto ((T_C - T)/T_C)^{\beta}$ governs the order parameter M just below the critical temperature (where β is the critical exponent), but this behaviour is more strongly affected by the finite size of the simulation because the singular behaviour at the phase transition only occurs in the thermodynamic limit, whereas in a finite system the divergence in the correlation length is curtailed and the phase transition is smoothed [32]. The correction to the theory of critical exponents in the limit of small systems is that $M \propto N^{-\beta/\nu}((T_C - T)/T_C)^{\beta}$ (whilst the values of the critical exponents are themselves unchanged) [23]. This correction gives the form of equation (11). The value of the critical exponent is confirmed using a log-log plot near the critical temperature to be $\beta = 0.29 \pm 0.02$ which is close to the value of approximately 0.33 quoted in ref. [32].

A theoretical understanding of finite size effects has been developed which suggests that the critical temperature in a finite system with N atoms should deviate from the value in the thermodynamic limit T_∞ by an amount $\delta T_C = aT_\infty N^{-1/\nu}$ where $a = 0.98$ [15, 23]. The result quoted above shows that this deviation is negligible in this simulation. Furthermore, all of the simulations in this project use at least 128 atoms, which would give predicted corrections of less than 2×10^{-3} K. We can therefore rest safely in the knowledge that the Monte Carlo simulations will reproduce experimental results such as monopole dynamics at the correct temperature scales.

4.2 Square ice

The 2D analogue of spin ice, known as 'square ice', was a useful system to study as preparation for simulating spin ice on the pyrochlore lattice. It consists of horizontally and vertically aligned Ising spins arranged in a square lattice with the analogue of the tetrahedron sites being the corners where the spin axes intersect (figure 3). Like spin ice, square ice obeys the spin ice Hamiltonian (2) and exhibits magnetic monopole excitations. For the sake of simplicity and computational efficacy I simulated square ice using only the first term of the Hamiltonian with $\nu_0/k_B = 1$ K, so that there was an energy cost to creating monopoles but the monopoles were non-interacting.

Figure 4 shows the internal energy of a square ice lattice with 16×16 unit cells (512 spins) and periodic boundary conditions in all directions cooled with 10^3 temperature steps and 50 Metropolis iterations per step from 10 K to 0.01 K. The system undergoes a transition[4] from a disordered paramagnetic regime (where dynamics are dominated by spin flips) to a 'spin ice' regime (where monopoles are sparse and dynamics are dominated by monopole propagation) at around 1K before reaching the spin ice ground state at around 0.1 K, mimicking the behaviour of spin ice. The ground state, which is shown in the schematic diagram in figure 3a, has all sites obeying the ice

[4] One might expect this transition to be a phase transition similar to the one in the standard 3D Ising model, but in fact there is no symmetry breaking involved, and a broad peak in the heat capacity is measured around the applicable Curie-Weiss temperature, rather than the sharp peak which would be seen in the standard 3D Ising model [5, 20].

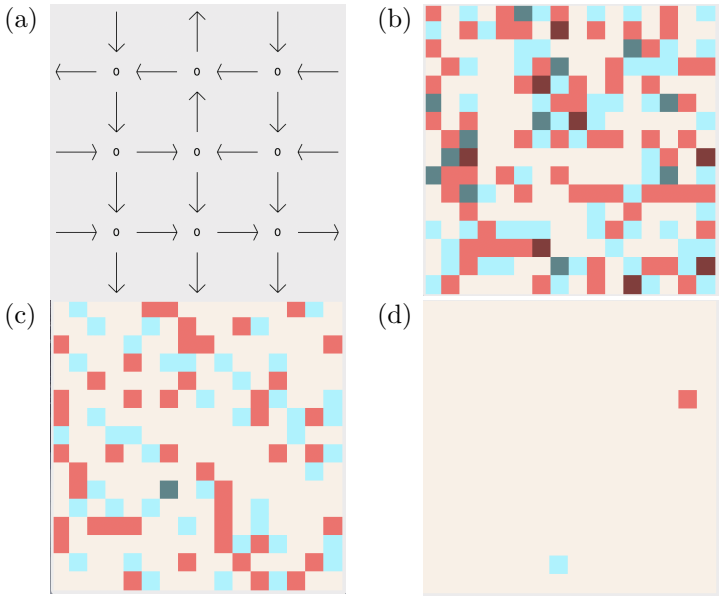

Figure 3: (a) Schematic plot of the ground state of square ice (in zero applied field). All the sites obey the ice rules and have zero magnetic charge, but there is no long range order. (b)-(d) Schematic plots of excitations during fast cooling of square ice at 10 K, 1 K and 0.01 K. Red and blue squares represent north and south poles respectively; doubly charged monopoles (sites where ice rules are doubly broken) are shown in darker colours. There is a paramagnetic regime at 10 K characterised by thermal spin flips which gives way to a ground state with two quenched defects (a monopole pair) at 0.01 K, with a transitional regime at around 1 K.

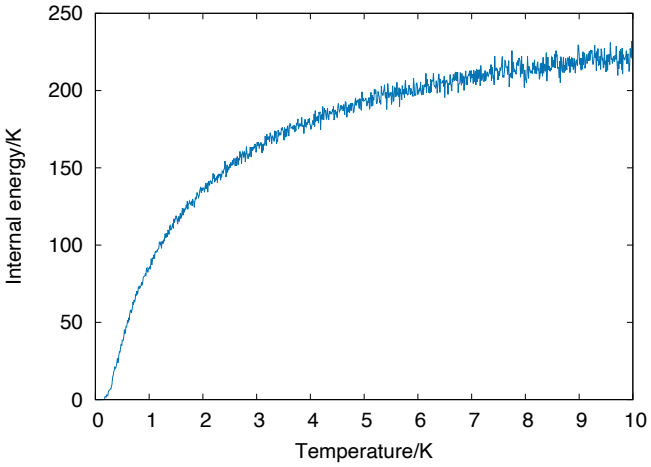

Figure 4: Internal energy of a square ice lattice undergoing simulated slow cooling plotted against temperature. A sharp drop around 1 K is associated with a transition to the spin ice regime. At very low temperature the internal energy levels off at zero when the ground state is reached.

rules with two spins pointing in and two pointing out but does not display any long range order, as is expected for spin ice in zero applied field [17]. Further schematic plots in figure 3 show the density of monopoles at various points in a similar cooling process with 10^2 temperature steps and 5 Metropolis iterations per step, where a disordered regime at high temperature gives way to a spin ice regime with low monopole density below about 1 K.

It was also interesting to look at the effects of the simulation parameters in the square ice lattice, such as the finite system size and the cooling rate. Whilst I have established in the discussion of the 3D simple cubic Ising magnet that finite size effects do not significantly affect the critical temperature and critical exponents, the topological constraints discussed previously (such as the presence of Dirac strings) exist in square ice and will increasingly hinder relaxation to equilibrium in larger systems at low temperature. Monopole pairs may only recombine by flipping a chain of spins along one of the Dirac strings, so if two monopole pairs come into contact in any other way they will be unable to recombine. Although this square ice simulation will not suffer from dynamical arrest as the monopoles are taken to be non-interacting, monopoles can still freeze into the lattice if they are unable to re-traverse the Dirac string in a certain number of temperature steps. Indeed, one observes that the system reaches the ground state at lower temperatures as the lattice size increases. Figure 5 shows the lattice side length l plotted against the temperature T_g where the ground state is reached. The fit suggests that a power law of the form $T_g = Cl^{-\gamma}$ applies (at least in the limit of small size) with $\gamma = 0.93 \pm 0.03$ and $C = (2.0 \pm 0.1)$ K. This demonstrates the general tendency of Monte Carlo simulations to display more quenching as the size is increased, and can be understood in spin ice terms as the lengths of the Dirac strings increasing with the size of the lattice, so that the chance of a monopole pair recombining by moving along a Dirac string in a certain number of cooling steps decreases.

These considerations would suggest that monopole quenching can be prevented by using enough Metropolis cooling steps for the generation and recombination of monopoles to remain in quasi-equilibrium as the sample is cooled, and that the number of steps required to cool the lattice without monopole quenching will increase with the lattice size. I investigated this by cooling a 28×28 square ice lattice from 10 K to 0.1 K using between 20 and 640 temperature steps T_s, and finding $N_{0.1}$, the number of monopoles remaining at that temperature (figure 5). Once again it is found that these quantities are related by a power law $N_{0.1} = (D/T_s)^{\delta}$ where $\delta = 0.53 \pm 0.08$ and $D = (0.16 \pm 0.03)$ K. Simulations such as this could in principle be used to determine the number of temperature steps needed for equilibrium thermodynamics to be valid so that physically accurate results could be obtained without the need for excessive computing power. For a large number of steps the power law governing $N_{0.1}$ should give way to a constant value equal to the equilibrium value[5]. It can be seen in these results that the curve may begin to level off at around one monopole, which suggests that this is close to the equilibrium value in which case ≈ 60 temperature steps per Kelvin of cooling (with 50 Metropolis iterations per step) should prevent monopole quenching and provide an accurate physical description, although clearly more data would be needed to confirm this in this particular case.

[5]A caveat is that both the real materials and the Monte Carlo simulations display 'glassy' behaviour which as I have mentioned explains how a residual entropy can exist close to absolute zero. In this regard, the simulation is physically accurate but does not actually reach equilibrium at very low temperature.

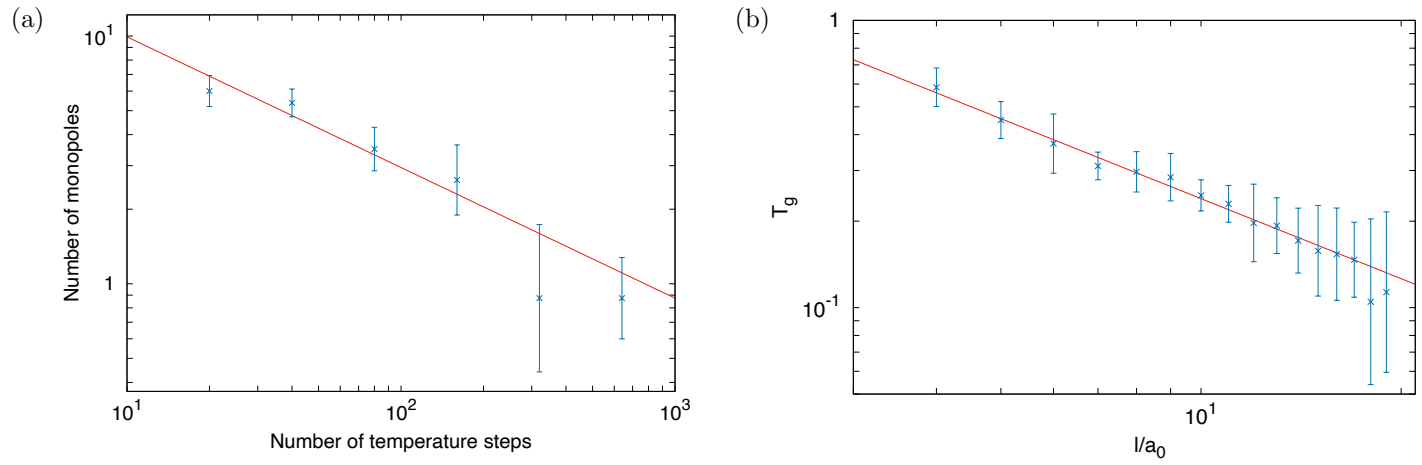

Figure 5: (a) Number of monopoles remaining at 0.1 K plotted against the number of cooling steps used. A power law may be a good approximation to describe the reduction in quenching as more cooling steps are used, but the number of monopoles should eventually tail off to the equilibrium (or quasi-equilibrium) value. (b) Temperature where the ground state is reached T_g plotted against the lattice size in units of the cubic diamond lattice constant a_0. This behaviour is not representative of equilibrium thermodynamics and is a result of the fact that more iterations of the algorithm are required to reach the ground state as the lattice size is increased.

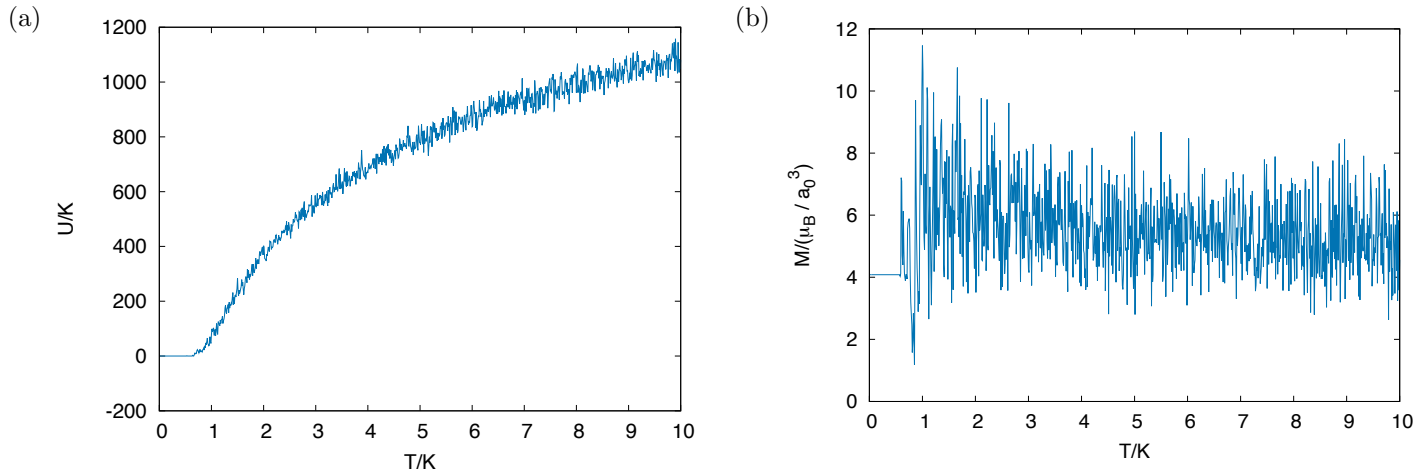

Figure 6: (a) Internal energy U of $Dy_2Ti_2O_7$ plotted against temperature T during cooling. The ground state persists up to almost 1 K followed by a region of linear increase, then a transition to the paramagnetic regime at about 2 K. (b) Magnetisation $M = |\mathbf{M}|$ during the same cooling procedure. There is a frozen magnetisation in the ground state, followed by a sharp increase in the spin ice regime (due to monopoles) followed by an eventual decay at high temperature. The magnetisation is always small (less than one spin magnetic moment per cubic unit cell), which is indicative of the lack of long range order.

4.3 3D spin ice

Finally, the general Ising model machinery was applied to spin ice compounds on the pyrochlore lattice in order to investigate the thermodynamic and magnetic properties in the spin ice regime. The full Hamiltonian was used with parameters[6] for $Dy_2Ti_2O_7$, so that the monopoles interacted Coulombically. Figure 6 shows the internal energy and magnetisation for a $4 \times 4 \times 4$ pyrochlore system (1024 spins) with periodic boundary conditions in all directions cooled with 10^3 temperature steps and 5 Metropolis iterations per step from 10 K to 0.01 K. The resulting ground state obeys the ice rules but displays no long-range order (figure 8). Just as in square ice, the internal energy displays a transition from the paramagnetic regime to the spin ice regime, at around 2 K. The magnetisation takes on a constant value in the ground state which is not unique thanks to the macroscopically degenerate ground state spin configuration and is seen to vary randomly in multiple independent simulations. As monopole excitations appear the magnetisation increases sharply before decaying back towards some other value at higher temperatures. This has hints of paramagnetic behaviour as seen in the 3D Ising model, although the magnetisation does not decay to zero but to some constant value which I found qualitatively to decrease with the lattice size: this is probably due to the fact that in a small lattice the spin dipole fields struggle to fully cancel due to the geometric constraints. This residual magnetisation is less than a single spin magnetic moment per cubic unit cell and would be expected to disappear in the thermodynamic limit.

There is no reason why a strongly magnetised ground state cannot be reached even in the macroscopic limit, but this would

[6] I used the parameters quoted in ref. [12].

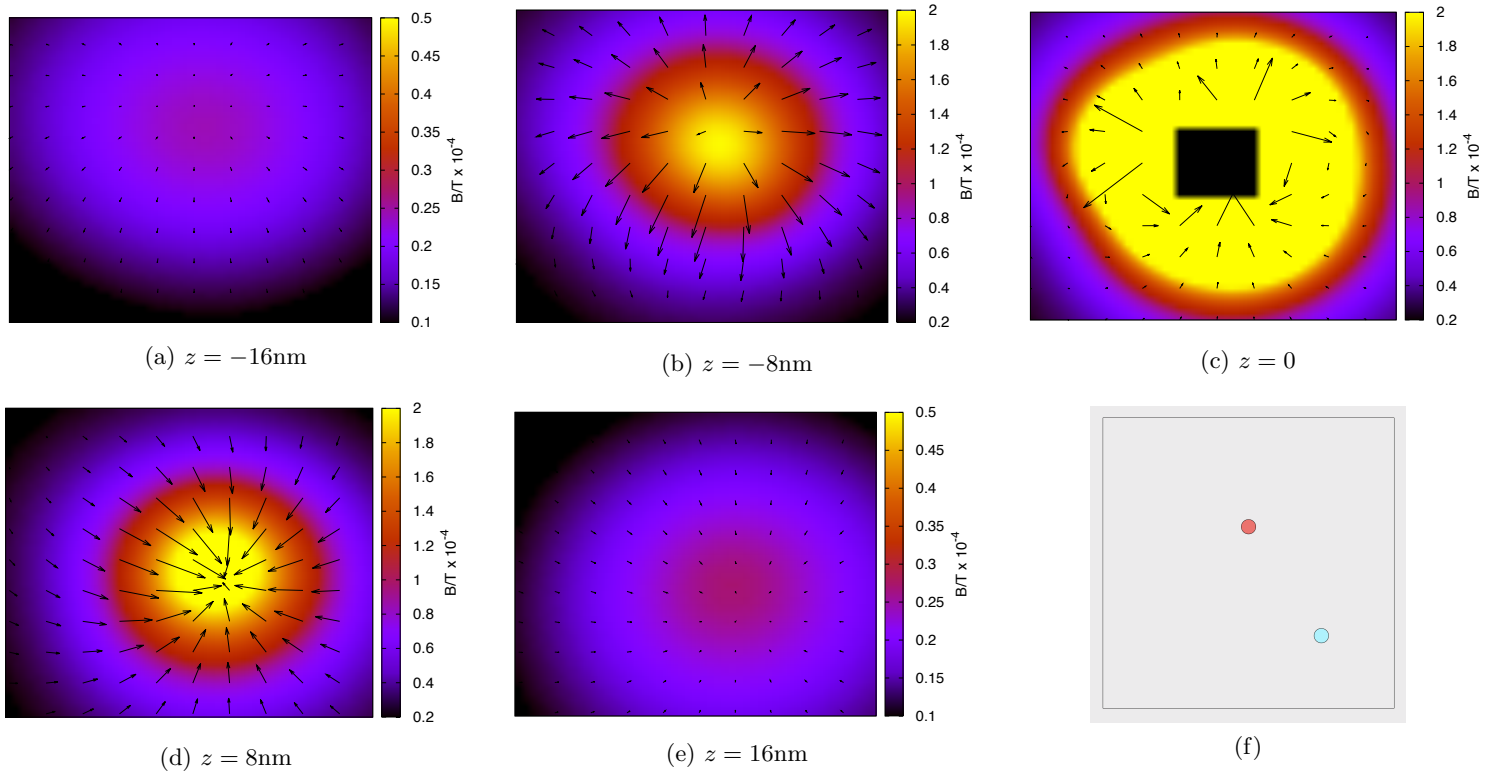

(a) $z = -16$nm (b) $z = -8$nm (c) $z = 0$

(d) $z = 8$nm (e) $z = 16$nm (f)

Figure 7: (a)-(e) Magnitude and direction of the stray field in the x-y plane above and below a cubic sample with side length 4 nm containing one monopole pair. Note that in (c) the arrow size has been reduced by a factor of 10. (f) Schematic plot showing the locations of the north (red) and south (blue) monopoles in the sample in the x-y plane (the south pole is below the north pole).

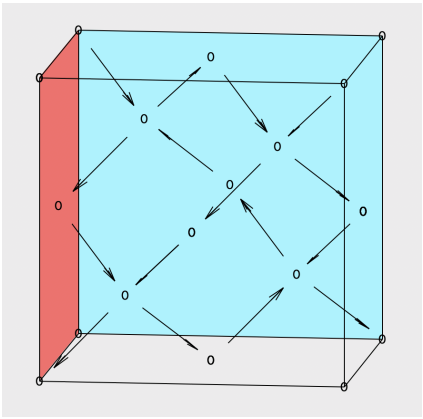

Figure 8: Schematic diagram of the spin ice ground state in a single unit cell within the simulated sample, with the numbers at the diamond lattice sites (tetrahedron centres) representing the monopole charge on the site. The pyrochlore tetrahedron outlines are not shown.

require at least some long range order which becomes exponentially less likely as N increases[7]. Thus the ground state magnetisation for real systems is expected to be negligible, and a signature magnetisation due to monopoles is expected to appear at low temperature in the spin ice regime. This signature will also be manifest in the stray field. Figure 7 shows the stray field in the x-y plane near a $4 \times 4 \times 4$ pyrochlore sample containing a single monopole pair. Evidence of a classical Coulomb field near the monopoles is observed, which provides a convincing qualitative demonstration of the theory of emergent magnetic monopoles in spin ice. This simulation also confirms that stray fields are important in spin ice and so would be expected to influence the results of μSR experiments as is argued in ref. [2].

4.4 Magnetic monopole noise

The experimental detection of single monopoles in spin ice remains beyond the reach of current technology, but the signature generation-recombination (GR) noise in the magnetisation (already seen during cooling in figure 6) has been measured using a SQUID device, providing insight into monopole dynamics in the spin ice regime [12, 22]. I used the $Dy_2Ti_2O_7$ simulation developed in the previous section with the full Hamiltonian (2) to simulate this monopole noise. The simulation consisted of cooling a $2 \times 2 \times 2$ lattice (128 spins) from 10 K to various temperatures between 1 K and 3.5 K using 100 cooling steps and 2 Metropolis iterations per step, before running 5000 Metropolis steps at fixed temperature and recording the magnetisation at each step[8]. The process was repeated independently ten times for each temperature and the mean power spectrum was taken.

[7] This discussion applies to the case of zero applied magnetic field, but when a field is applied a phase transition to an ordered state with a magnetisation is observed [17]. This corresponds to a monopole gas-liquid transition [7].

[8] It would have been preferable to use a larger lattice and more steps as in previous simulations, but this was not possible as I was working at the limits of the computation power available on a personal computer. Typically supercomputers are used to carry out these simulations [21]. The only aspect on which I could not compromise was the number of time steps used to measure the noise at fixed temperature so that the full range of dynamics was captured.

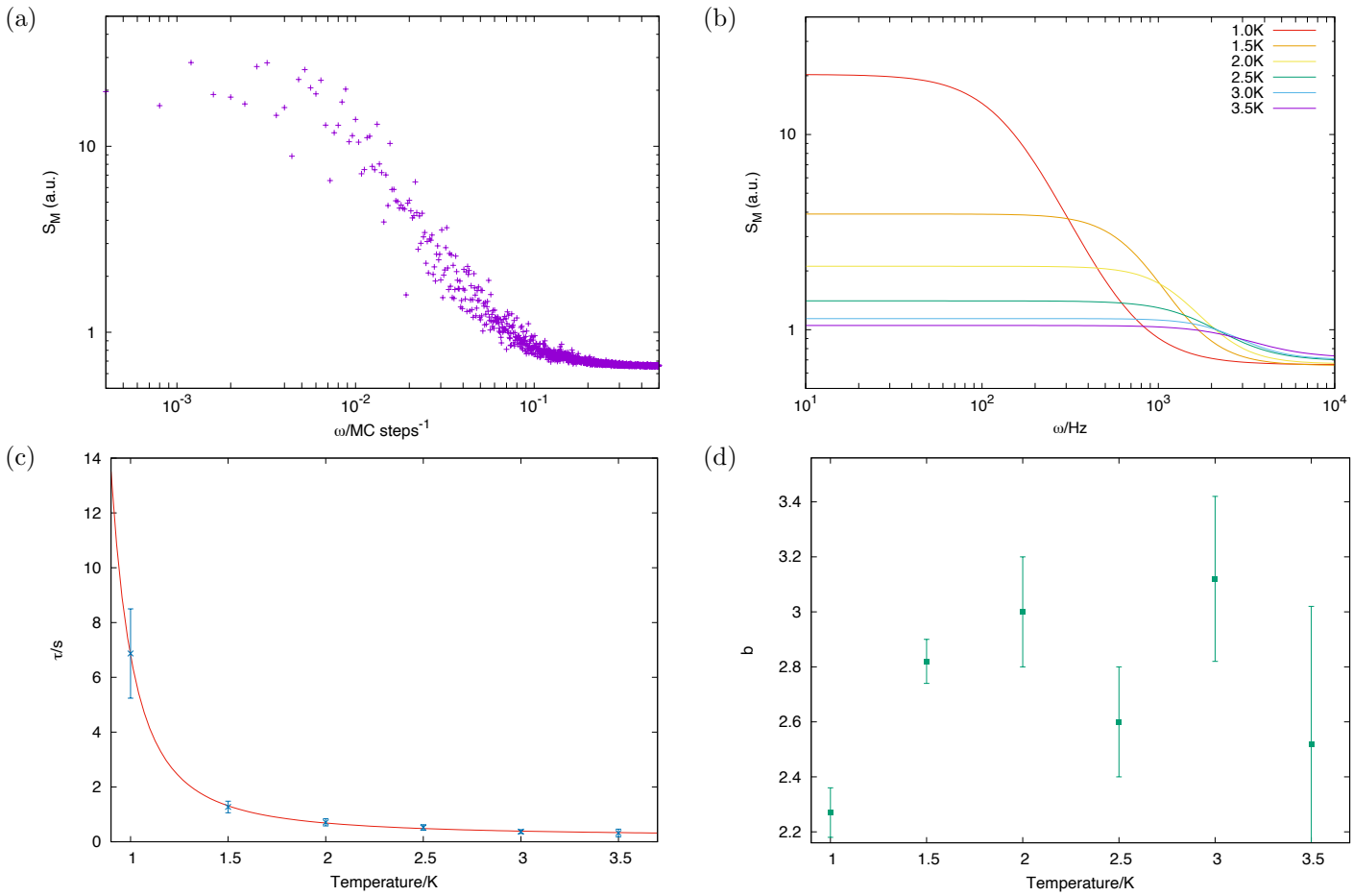

Figure 9: Results of magnetic monopole noise simulations, observed in fluctuations in the magnetisation, between 1 K and 3.5 K. (a) Raw power spectral density S_M data at 1 K. The constant and power law regimes can be seen, as well as a further tail-off due to the vertical shift resulting from Nyquist noise (which was removed by fitting the tail to a constant). The curve is broadened significantly by additional noise due to monopole motion, which could be reduced by averaging over more independent simulations. It is likely that errors were introduced by the lack of points in the low frequency regime; to remedy this data would have to be taken over longer periods of time (requiring much more computing power). (b) Fits to power spectral density data using equation (8) for various temperatures in the range. A typical slowing in dynamics can be seen as the temperature is decreased. (c) Characteristic generation-recombination time constants obtained from the fits in (b), fitted to a VTF law (13). (d) Values of b obtained from the fits in (b). The values quantitatively disagree with values obtained by other authours, and there is no clear trend.

Figure 9b shows the fits to the power spectral density plotted at different temperatures. The behaviour of the power spectral density consists of a constant regime at low frequencies and a power law regime at high frequencies, which are the signature features of the Langevin monopole plasma with a characteristic GR timescale τ.

It proved difficult to fit the noise to a curve of the form in equation (8) because additional noise was produced by the motion of monopoles in the system which were not undergoing generation and recombination [22], which broadened the power spectrum curve significantly. It would be possible to reduce this effect by averaging over many more independent simulations, but the computing power required for this was not available. Furthermore, for simulations at higher temperatures some features began to be cut off by the Nyquist frequency at 0.5 MC steps^{-1}. The alternative approach used was to fit the constant and power law regimes separately: since for $b > 0$ $\lim_{\omega\to 0}\left(a\tau/(1+(\omega\tau)^b)\right) = a\tau$ and $\lim_{\omega\to\infty}\left(a\tau/(1+(\omega\tau)^b)\right) = (a\tau/\omega\tau)^b$ one can use the fits $S = a\tau$ at low frequency and $\log(S) = \log(a\tau) - b\log(\tau) - b\log(\omega)$ at high frequency. A constant vertical shift in S present due to Nyquist noise [12, 30] was removed by fitting the asymptotic high frequency behaviour of the curve to a constant and subtracting. The values of b and τ were obtained in this way and are plotted in figure 9. The time constants were converted into seconds using the Monte Carlo step calibration in ref. [12] which was obtained by comparison with experimental measurements and gives 1 MC step $= (83 \pm 11)$ μs.

Since monopole GR is a thermally activated process, one may expect the time constant to be governed by the Arrhenius law

$$\tau = \tau_0 \exp\left(\frac{T_a}{T}\right) \tag{12}$$

where $k_B T_a$ is the energy required to create a monopole pair (the activation energy). However, the behaviour is in fact super-Arrhenius, with τ increasing faster than an exponential on cooling, and whilst some authours have tried to model τ using an Arrhenius law with a varying energy barrier [19, 24, 31], the

Vogel-Tammann-Fulcher (VTF) law

$$\tau = \tau_0 \exp\left(\frac{DT_0}{(T - T_0)}\right) \tag{13}$$

turns out to be a far better fit to experimental data over the full temperature range of interest [11, 13, 20]. This empirical relation, which is often successfully used to describe glassy systems, has exponential behaviour similar to the Arrhenius law (12) but with the parameter D denoting the so-called 'fragility', with a larger fragility (smaller D) denoting a faster arrest in the dynamics in comparison to the Arrhenius law [9]. In spin ice, this deviation from the thermally activated behaviour expected of a free monopole plasma can be attributed to the fact that magnetic Coulomb interactions and topological constraints affect monopole dynamics and can often hinder monopole GR.

	Value obtained from fit	Value in ref. [12]
D	7.2 ± 2.7	11 ± 6.8
T_0/K	0.35 ± 0.08	0.25 ± 0.1
τ_0/ms	0.15 ± 0.02	0.098 ± 0.019

Table 2: Summary of VTF fitting parameters (equation (13))

The dynamics simulated here closely obey a VTF law (figure 9c) and the parameters obtained are summarised in table 2 alongside experimental values obtained in ref. [12]. The parameters obtained are similar but T_0 in particular does not agree within the error bounds. The simulation here predicts that the GR time constant increases slightly more slowly with temperature between 1 K and 4 K than it is observed to in ref. [12]. However, the apparent success of the VTF fit could be misleading because comparatively few data points were used; in ref. [12] there are many more points below 2 K and the fit agrees much better in this region than above 2 K, whereas the fit presented here is mostly based on points above 2 K. It could be that this partially accounts for some of the discrepancies in table 2. Furthermore, discrepancies between Monte Carlo simulations of spin ice dynamics and experiments have been reported in the past [31]. It has also been noted that simulations often predict that dynamics of glassy systems slow down more quickly with temperature than is observed in experiments because simulations cannot typically cover as large a timescale as experiments, so simulated systems are unable to explore as much of the phase space and begin to show off-equilibrium behaviour at higher temperatures [9]. Other effects which may contribute to these discrepancies include the fact that spin flips may be better described as quantum tunnelling phenomena rather than classical spin flips; a proper computational treatment of this has not yet been achieved [11, 13].

Turning attention to the power law behaviour at high frequencies, one sees in figure 9d that there is a significant deviation from the Debye-Lorentzian value $b = 2$ predicted for the free monopole plasma. This is not surprising in itself because topological constraints and Coulomb interactions will cause the motion of monopoles to become correlated, and the effects of those correlations on the power law drop-off remains unclear [11]. Experiments show that $b < 2$ and decreases as the temperature increases[9]; simulations in previous work show the same trend but do not quantitatively agree with experiment [11, 12, 21]. This lack of agreement has been attributed to the fact that additional correlations from next nearest neighbour superexchange interactions have not been included in simulations [11]. However, the results presented here, which show that $b > 2$ (with no clear trend), disagree starkly with both experiment and previous simulations. One possible reason for this is that most simulations reported in the literature use loop algorithms, which consist of identifying loops of spins pointing in the same sense of the kind described by Pauling [28] and proposing flipping the whole loop, in addition to single spin flips at each Metropolis step [21, 25]. This is designed to encourage relaxation to equilibrium in the ground state or free propagation of monopoles in low-lying excited states. It is possible that this algorithm would allow the system to explore more of the phase space in a given number of time steps, leading to more dynamics at lower timescales, which would reduce the speed of the power law drop-off. However, using this method in these simulations was not feasible with the available computing power.

5 Conclusions

In this project I have applied Monte Carlo simulations to three magnetic systems: the standard 3D Ising model on the simple cubic lattice, the hypothetical 2D material square ice and the real spin ice material $Dy_2Ti_2O_7$. In the first I successfully demonstrated the behaviour of the order parameter near the phase transition, obtained the critical temperature and critical exponent β and achieved quantitative agreement with other similar computational work. In the second I recreated simple characteristic spin ice properties such as the macroscopically degenerate ground state and the transition to the spin ice regime. I also investigated the effects of the finite simulation size and number of iterations of the Metropolis algorithm on the convergence to thermodynamic equilibrium in order to understand the limitations of applying Monte Carlo simulations to real systems. Lastly, in simulations of $Dy_2Ti_2O_7$ I demonstrated the properties of the ground state, internal energy, magnetisation and stray field, the latter of which revealed a signature of magnetic monopole excitations. I also successfully reproduced the characteristic monopole generation-recombination noise evident in fluctuations in the magnetisation and obtained a characteristic time constant governing monopole dynamics with a typical temperature dependence.

Perhaps the biggest open issue in the study of spin ice is the question of correlated magnetic monopole dynamics: how they can be accurately represented in Monte Carlo simulations and how effects such as next nearest neighbour superexchange interactions and quantum tunnelling spin flips can be accounted for. More specifically to this project, it would be interesting to see what effect the inclusion of loop algorithms would have on the simulation behaviour, and especially on parameter b in equation (8) (these algorithms have been well studied). Other issues include the lack of a satisfactory theoretical description of edge effects, although this has not hindered experimental work which has been done on spin ice materials [21].

[9] I have previously stated that there is a transition from a paramagnetic regime dominated by thermal spin flips to a spin ice regime with sparse monopoles at around 2 K, so perhaps it is unsurprising that the monopole picture becomes a worse approximation at higher temperatures. I chose this temperature range in order to obtain comparable results to ref. [12]; a new generation of SQUID devices operating at low temperature will be needed to obtain experimental data further into the spin ice regime [11].

References

[1] Blundell, S. J. (2001). *Magnetism in Condensed Matter* (1st ed.). Oxford: Oxford University Press.

[2] Blundell, S. J. (2012). Monopoles, magnetricity and the stray field from spin ice. *Physical Review Letters*, *108*, 147601.

[3] Blundell, S. J. & Blundell, K. M. (2010). *Concepts in Thermal Physics* (2nd ed.). Oxford: Oxford University Press.

[4] Bramwell, S. T., Giblin, S. R., Calder, S., Aldus, R., Prabhakaran, D., & Fennell, T. (2009). Measurement of the charge and current of magnetic monopoles in spin ice. *Nature*, *461*, 956.

[5] Bramwell, S. T. & Gingras, M. J. P. (2001). Spin ice state in frustrated magnetic pyrochlore materials. *Science*, *294*, 1495.

[6] Cabrera, B. (1982). First results from a superconductive detector for moving magnetic monopoles. *Physical Review Letters*, *48*, 1378.

[7] Castelnovo, C., Moessner, R., & Sondhi, S. L. (2008). Magnetic monopoles in spin ice. *Nature*, *451*, 42.

[8] Castelnovo, C., Moessner, R., & Sondhi, S. L. (2010). Thermal quenches in spin ice. *Physical Review Letters*, *104*, 107201.

[9] Cavagna, A. (2009). Supercooled liquids for pedestrians. *Physics Reports*, *476*, 51.

[10] Dirac, P. A. M. (1931). Quantised singularities in the electromagnetic field. *Proceedings of the Royal Society A*, *133*, 60.

[11] Dusad, R. (2021). *Magnetic monopole noise*. PhD thesis, Cornell University.

[12] Dusad, R., Kirschner, F. K. K., Hoke, J. C., Roberts, B. R., Eyal, A., Flicker, F., Luke, G. M., Blundell, S. J., & Davis, J. C. S. (2019). Magnetic monopole noise. *Nature*, *571*, 234.

[13] Eyvazov, A. B., Dusad, R., Munsie, T. J. S., Dabkowska, H. A., Luke, G. M., Kassner, E. R., Davis, J. C. S., & Eyal, A. (2018). Common glass-forming spin-liquid state in the pyrochlore magnets $Dy_2Ti_2O_7$ and $Ho_2Ti_2O_7$. *Physical Review B*, *98*, 214430.

[14] Fennell, T., Petrenko, O. A., Fak, B., Bramwell, S. T., Enjalran, M., Kavors'kii, T., Gingras, M. J. P., Melko, R. G., & Balakrishnan, G. (2004). Neutron scattering investigation of the spin ice state in $Dy_2Ti_2O_7$. *Physical Review B*, *70*, 134408.

[15] Ferrenberg, A. M., Xu, J., & Landau, D. P. (2018). Pushing the limits of monte carlo simulations for the three-dimensional ising model. *Physical Review E*, *97*, 043301.

[16] Giauque, W. F. & Stout, J. W. (1936). The entropy of water and the third law of thermodynamics. the heat capacity of ice from 15 to 273 K. *Journal of the American Chemical Society*, *58*, 1144.

[17] Harris, M. J., Bramwell, S. T., McMorrow, D. F., Zeiske, T., & Godfrey, K. W. (1997). Geometrical frustration in the ferromagnetic pyrochlore $Ho_2Ti_2O_7$. *Physical Review Letters*, *79*, 2554.

[18] Jackson, J. D. (1975). *Classical Electrodynamics* (2nd ed.). New York; Chichester: Wiley.

[19] Jaubert, L. D. C. & Holdsworth, P. C. W. (2011). Magnetic monopole dynamics in spin ice. *Journal of Physics: Condensed Matter*, *23*, 164222.

[20] Kassner, E. R., Eyvazov, A. B., Pichler, B., Munsie, T. J. S., Dabkowska, H. A., Luke, G. M., & Davis, J. C. S. (2015). Supercooled spin liquid state in the frustrated pyrochlore $Dy_2Ti_2O_7$. *Proceedings of the National Academy of Sciences*, *112*, 8549.

[21] Kirschner, F. K. K. (2018). *Computational and experimental studies of exotic magnets and superconductors*. PhD thesis, University of Oxford.

[22] Kirschner, F. K. K., Flicker, F., Yacoby, A., Yao, N. Y., & Blundell, S. J. (2018). Proposal for the detection of magnetic monopoles in spin ice via nanoscale magnetometry. *Physical Review B*, *97*, 140402(R).

[23] Landau, D. P. (1976). Finite size behaviour of the simple cubic ising lattice. *Physical Review B*, *14*, 255.

[24] Matsuhira, K., Paulsen, C., Lhotel, E., Sekine, C., Hiroi, Z., & Takagi, S. (2011). Spin dynamics at very low temperature in spin ice $Dy_2Ti_2O_7$. *Journal of the Physical Society of Japan*, *80*, 123711.

[25] Melko, R. G. & Gingras, M. J. P. (2004). Monte carlo studies of the dipolar spin ice model. *Journal of Physics: Condensed Matter*, *16*, 1277(R).

[26] Metropolis, N., Rosenbluth, A. W., Rosenbluth, M. N., Teller, A. H., & Teller, E. (1953). Equation of state calculations by fast computing machines. *Journal of Chemical Physics*, *21*, 1087.

[27] Morris, D. J. P., Tennant, D. A., Grigera, S. A., Klemke, B., Castelnovo, C., Moessner, R., Czternasty, C., Meissner, M., Rule, K. C., Hoffman, J.-U., Kiefer, K., Gerischer, S., Slobinsky, D., & Perry, R. S. (2009). Dirac strings and magnetic monopoles in the spin ice $Dy_2Ti_2O_7$. *Science*, *326*, 411.

[28] Pauling, L. (1935). The structure and entropy of ice and of other crystals with some randomness of atomic arrangement. *Journal of the American Chemical Society*, *57*, 2680.

[29] Ramirez, A. P., Hayashi, A., Cava, R. J., Siddharthan, R., & Shastry, B. S. (1999). Zero-point entropy in 'spin ice'. *Nature*, 333.

[30] Raquet, B. (2001). Electronic noise in magnetic materials and devices. In *Spin Electronics*. New York: Springer.

[31] Yaraskavitch, L. R., Revell, H. M., Meng, S., Ross, K. A., Noad, H. M. L., Dabkowska, H. A., Gaulin, B. D., & Kycia, J. B. (2012). Spin dynamics in the frozen state of the dipolar spin ice material $Dy_2Ti_2O_7$. *Physical Review B*, *85*, 020410.

[32] Yeomans, J. M. (1992). *Statistical Mechanics of Phase Transitions* (1st ed.). Oxford: Oxford University Press.